Juansilvaite, $Na_5Al_3[AsO_3(OH)]_4[AsO_2(OH)_2]_2(SO_4)_2 \cdot 4H_2O$, a new arsenate-sulfate from the Torrecillas mine, Iquique Province, Chile

Anthony R. Kampf[1,*], Barbara P. Nash[2], Maurizio Dini[3] and Arturo A. Molina Donoso[4]

[1] Mineral Sciences Department, Natural History Museum of Los Angeles County, 900 Exposition Boulevard, Los Angeles, CA 90007, USA
[2] Department of Geology and Geophysics, University of Utah, Salt Lake City, Utah 84112, USA
[3] Pasaje San Agustin 4045, La Serena, Chile
[4] Los Algarrobos 2986, Iquique, Chile

ABSTRACT

The new mineral juansilvaite (IMA2015-080), $Na_5Al_3[AsO_3(OH)]_4[AsO_2(OH)_2]_2(SO_4)_2 \cdot 4H_2O$, was found at the Torrecillas mine, Iquique Province, Chile, where it occurs as a secondary alteration phase in association with anhydrite, canutite, halite, sulfur and a mahnertite-like phase. Juansilvaite occurs as bright pink blades up to ~0.5 mm long grouped in tightly intergrown radial aggregates and also as opaque dull pale pink rounded aggregates. Blades are flattened on {001}, elongated on [100] and exhibit the forms {001}, {111} and {20$\bar{1}$}. Crystals are transparent, with vitreous lustre and white streak. The Mohs hardness is ~ 2½, tenacity is brittle and fracture is irregular. Cleavage is very good on {001}. The measured density is 3.01(2) g cm^{-3} and the calculated density is 3.005 g cm^{-3}. Optically, juansilvaite is biaxial (+) with $\alpha = 1.575(1)$, $\beta = 1.597(1)$, $\gamma = 1.623(1)$ and $2V = 86(1)°$ (measured in white light). Dispersion is $r < v$, slight, and the orientation is $X = \mathbf{b}$; $Z \wedge \mathbf{c} = 27°$ in the obtuse angle β. The pleochroism is $X > Y \approx Z$ in shades of pale pink. The mineral is slowly soluble in dilute HCl at room temperature. The empirical formula, determined from electron-microprobe analyses, is $Na_{4.95}Al_{2.28}Fe^{3+}_{0.50}Mn^{3+}_{0.21}Cu_{0.04}As_{5.92}S_{1.83}O_{36}H_{17.37}$. Juansilvaite is monoclinic, $C2/c$, $a = 18.1775(13)$, $b = 8.6285(5)$, $c = 18.5138(13)$ Å, $\beta = 90.389(6)°$, $V = 2903.7(3)$ Å^3 and $Z = 4$. The eight strongest powder X-ray diffraction lines are [d_{obs} Å(I)(hkl)]: 9.25(100)(002), 7.20(34)($\bar{1}$11), 4.545(34)(400), 3.988(39)($\bar{1}$14), 3.363(42)(314), 3.145(66)($\bar{5}$12,420), 2.960(68)($\bar{4}$22,422) and 2.804(33)(131,$\bar{4}$23). The structure of juansilvaite ($R_1 = 3.82\%$ for 2040 $F_o > 4\sigma F$ reflections) contains layers made up of alternating corner-linked Al–O octahedra and acid-arsenate tetrahedra. Sodium cations occur both peripheral to the layers and within cavities in the layers. An SO_4 tetrahedron and an H_2O group also are in the interlayer region.

Introduction

The Torrecillas mine, in the northern Atacama Desert of Chile, is a small, long-inactive arsenic mine. Over the last several years, our investigations of the minerals of this unusual deposit have yielded many new and potentially new mineral species. To date, the descriptions of six new minerals have been published: leverettite (Kampf *et al.*, 2013*a*), magnesiokoritnigite (Kampf *et al.*, 2013*b*), torrecillasite (Kampf *et al.*, 2014*a*), canutite (Kampf *et al.*, 2014*b*), chongite (Kampf *et al.*, 2016*a*) and gajardoite (Kampf *et al.*, 2016*b*). Herein, we describe the seventh new mineral from the Torrecillas mine, juansilvaite. Several other potentially new minerals are still under study.

The name juansilvaite honours Juan Silva Aguirre (1939–2012). Mr. Silva was a prominent Chilean mining engineer and among Chile's most successful mining entrepreneurs. He was responsible for the development and operation of several important mines and a myriad of smaller ones in the Copiapo, Tierra Amarilla and Vallenar areas of the Atacama Region. He professed that his principle motivation was to create employment opportunities for the people of his beloved Atacama Desert.

The new mineral and the name have been approved by the International Mineralogical Association (IMA2015-080, Kampf *et al.*, 2015). The description is based upon four cotype specimens that are deposited in the collections of the Natural History Museum of Los Angeles County, 900 Exposition Boulevard, Los Angeles, CA 90007, USA, catalogue numbers 65605, 65606, 65607 and 65608.

Occurrence

The Torrecillas mine is located on Torrecillas Hill, Iquique Province, Tarapacá Region, Chile (approximately 20°58'13''S, 70°8'17''W). Four different rock units are exposed on the hill. The Coastal Range Batholith (mainly gabbros) extends from the seashore to the Pan-American Road along the base of Torrecillas Hill. At the foot of Torrecillas Hill is a small area of contact metamorphic rocks in which garnet crystals occur in metamorphosed shales. Higher on the hill, the rocks are predominantly andesites and porphyritic lavas of the Jurassic La Negra Formation. The Torrecillas deposit, in which the new mineral is found, consists of two main veins rich in secondary arsenic and copper minerals that intersect metamorphosed marine shales and lavas. These mineralized veins are genetically related to the aforementioned andesites and porphyritic lavas of the Jurassic La Negra Formation. More information on the geology and mineralogy of the area is provided by Gutiérrez (1975).

The rare secondary chlorides, arsenates and arsenites have been found at three main sites on the hill: an upper pit measuring ∼8 m long and 3 m deep, a lower pit ∼100 m from the upper pit and measuring ∼5 m long and 3 m deep, and a mine shaft adjacent to the lower pit and lower on the hill. Juansilvaite was collected from a small outcrop near the upper pit by a collecting party consisting of three of the authors (ARK, MD and AAMD) along with Jochen Schlüter and Joe Marty in February 2014.

The new mineral is a secondary alteration phase occurring in association with anhydrite, canutite,

halite, sulfur and a mahnertite-like phase. The secondary assemblages at the Torrecillas deposit are interpreted as having formed from the oxidation of native arsenic and other As-bearing primary phases, followed by later alteration by saline fluids derived from evaporating meteoric water under hyperarid conditions (*cf*. Cameron *et al.*, 2007).

Physical and optical properties

Juansilvaite occurs as bright pink blades to ∼0.5 mm long grouped in tightly intergrown radial aggregates (Fig. 1) and also as dull pale pink rounded aggregates. Blades are flattened on {001}, elongated on [100] and exhibit the forms {001}, {111} and {20$\overline{1}$} (Fig. 2). No twinning was observed. Juansilvaite crystals are transparent with vitreous lustre and white streak. The mineral does not fluoresce in longwave or shortwave ultraviolet light. The Mohs hardness is ∼2½, based on scratch tests. The tenacity is brittle and the fracture is irregular. Cleavage is very good on {001}. The density measured by flotation in a mixture of methylene iodide and toluene is 3.01(2) g cm^{-3} and the calculated density is 3.005 g cm^{-3}. Optically, juansilvaite is biaxial (+) with $\alpha = 1.575(1)$, $\beta = 1.597(1)$ and $\gamma = 1.623(1)$ measured in white light. The 2V measured by direct conoscopic observation using a spindle stage is 86(1)°. The calculated 2V is 86.5°. Dispersion is $r < v$, slight. The optical orientation is $X = \mathbf{b}$; $Z \wedge \mathbf{c} = 27°$ in the obtuse angle β. The pleochroism is $X > Y \approx Z$ in shades of pale pink. The mineral is slowly soluble in dilute HCl at room temperature.

Composition

Quantitative analyses (10 points on five crystals) were performed at the University of Utah using a Cameca SX-50 electron microprobe with four wavelength-dispersive spectrometers utilizing *Probe for EPMA* software. Analytical conditions were 15 kV accelerating voltage, 20 nA beam current and a beam diameter of 15 μm. Juansilvaite is notably unstable under the electron beam, exhibiting very significant damage during the course of analyses despite the defocused beam. Arsenic, Na, S, Fe and Al were corrected for time-dependent variation in intensity during each spot analysis. Counting times were 20 s on peak and 10 s on + and – background. No other elements were detected by electron dispersive spectroscopy. Other probable elements were sought, but none
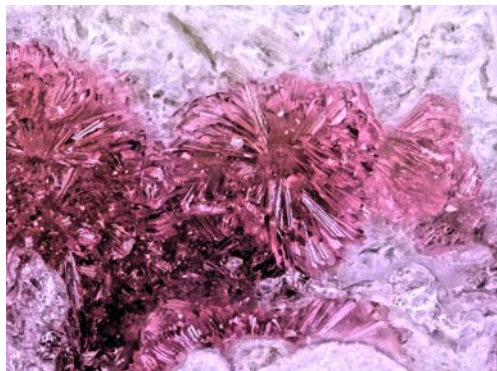
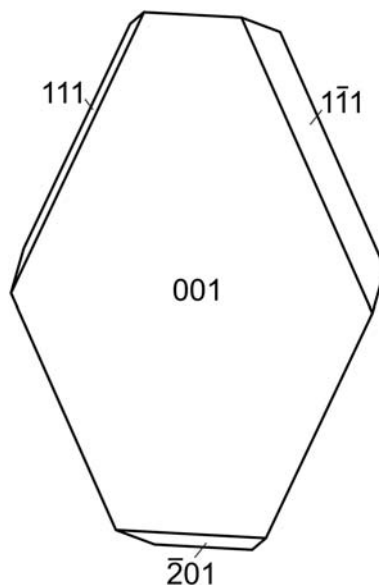FIG. 1. Juansilvaite crystals with halite on anhydrite. Field of view = 0.83 mm across.

FIG. 2. Crystal drawing of juansilvaite, clinographic projection in non-standard orientation, [100] vertical.

were above the detection limits. Raw X-ray intensities were corrected for matrix effects with a $\phi(\rho z)$ algorithm (Pouchou and Pichoir, 1991). Because insufficient material was available for a direct determination of H_2O, the amount of water was calculated on the basis of $Al + Fe + Mn = 3$ atoms per formula unit (apfu), charge balance and $O = 36$ apfu, as determined by the crystal structure analysis (see below). Analytical data are given in Table 1. The low analytical total is attributed to the instability of the mineral under the electron beam.

The empirical formula is $Na_{4.95}Al_{2.28}Fe^{3+}_{0.50}Mn^{3+}_{0.21}$ $Cu_{0.04}As_{5.92}S_{1.83}O_{36}H_{17.37}$. The simplified structural formula is $Na_5Al_3[AsO_3(OH)]_4[AsO_2(OH)_2]_2$ $(SO_4)_2 \cdot 4H_2O$, which requires Na_2O 11.90, Al_2O_3 11.75, As_2O_5 52.97, SO_3 12.30, H_2O 11.07, total 100 wt.%. The Gladstone-Dale compatibility $1 - (K_p/K_c)$ for the empirical formula is 0.013 in the range of superior compatibility (Mandarino, 2007).

X-ray crystallography and structure refinement

Both powder and single-crystal X-ray studies were carried out using a Rigaku R-Axis Rapid II curved imaging plate microdiffractometer, with monochromatic $MoK\alpha$ radiation. For the powder-diffraction study a Gandolfi-like motion on the ϕ and ω axes was used to randomize the sample and observed d-valves and intensities were derived by profile fitting using *JADE 2010* software (Materials Data, Inc.). The powder data presented in Table 2 show

TABLE 1. Analytical data (wt.%) for juansilvaite.

Constituent	Mean	Range	SD	Standard
Na_2O	11.35	10.85–12.20	0.46	albite
CuO	0.24	0.13–0.40	0.10	Cu metal
Al_2O_3	8.61	7.39–10.15	0.99	YAG
Mn_2O_3	1.24	0.56–2.34	0.72	rhodonite
Fe_2O_3	2.97	0.16–5.89	2.13	hematite
As_2O_5	50.34	48.47–54.74	2.06	syn. GaAs
SO_3	10.82	8.70–12.28	1.30	celestine
H_2O^*	11.57			
Total	97.14			

*Calculated on the basis of $Al + Fe + Mn = 3$ apfu, charge balance and $O = 36$ apfu.

TABLE 2. Powder X-ray data for juansilvaite. Only calculated lines with $I_{calc} > 1$ are included.

I_{obs}	d_{obs}	d_{calc}	I_{calc}	h k l
100	9.25	9.2567	100	0 0 2
		9.0885	7	2 0 0
34	7.20	7.1916	37	$\bar{1}$ 1 1
9	6.45	6.4633	7	2 0 2
18	4.837	4.8453	7	$\bar{1}$ 1 3
		4.8316	8	1 1 3
		4.7831	3	3 1 1
		4.6283	3	0 0 4
34	4.545	4.5443	25	4 0 0
		4.3609	3	3 1 2
12	4.313	4.3143	10	0 2 0
		4.2017	4	0 2 1
26	4.120	4.1357	13	$\bar{2}$ 0 4
		4.1131	4	2 0 4
		4.0902	4	$\bar{4}$ 0 2
		4.0683	5	4 0 2
43	3.988	3.9848	39	$\bar{1}$ 1 4
		3.9104	7	0 2 2
26	3.824	3.8161	25	$\bar{2}$ 2 1
		3.5958	3	$\bar{2}$ 2 2
5	3.544	3.5359	4	0 2 3
		3.3929	2	$\bar{3}$ 1 4
42	3.363	3.3741	34	3 1 4
		3.2996	3	$\bar{2}$ 2 3
		3.2931	5	5 1 1
		3.2537	3	$\bar{4}$ 0 4
		3.2317	4	4 0 4
66	3.145	3.1566	33	$\bar{5}$ 1 2
		3.1288	29	4 2 0
		3.0856	4	0 0 6
		2.9855	8	$\bar{2}$ 2 4
		2.9747	4	$\bar{3}$ 1 5
68	2.960	2.9683	13	$\bar{4}$ 2 2
		2.9599	38	4 2 2
		2.9521	2	$\bar{5}$ 1 3
		2.9366	2	5 1 3
26	2.879	2.9158	10	2 0 6
		2.8718	12	$\bar{1}$ 1 6
		2.8661	13	1 1 6
33	2.804	2.8075	11	1 3 1
		2.7959	22	$\bar{4}$ 2 3
22	2.719	2.7220	15	$\bar{5}$ 1 4
		2.7166	7	$\bar{1}$ 3 2
		2.7058	2	5 1 4
		2.6883	2	$\bar{2}$ 2 5
		2.6263	2	$\bar{3}$ 1 6
		2.6133	6	3 1 6
11	2.598	2.5977	2	$\bar{4}$ 2 4
		2.5865	3	4 2 4
8	2.551	2.5720	7	3 3 1
		2.5427	6	$\bar{6}$ 0 4
		2.4997	2	3 3 2
8	2.474	2.4793	5	6 2 0
		2.4592	5	$\bar{6}$ 2 1
7	2.405	2.4158	3	2 2 6
		2.3982	4	$\bar{6}$ 2 2
2	2.328	2.3390	2	$\bar{3}$ 1 7
		2.3282	3	3 1 7
		2.3142	2	0 0 8
		2.2721	2	8 0 0
8	2.251	2.2629	2	3 3 4
		2.2527	3	1 3 5
		2.2390	5	2 0 8
		2.2202	2	$\bar{1}$ 1 8
6	2.206	2.2032	2	8 0 2
		2.1918	3	4 2 6
		2.1855	2	2 2 7
		2.1214	3	$\bar{5}$ 3 3
8	2.1035	2.1015	5	$\bar{3}$ 1 8
		2.0911	2	$\bar{1}$ 3 6
7	2.0469	2.0476	7	$\bar{2}$ 4 2
4	1.9724	1.9846	4	3 3 6
		1.9621	4	8 2 2
		1.9542	4	9 1 1
15	1.9408	1.9423	2	$\bar{7}$ 1 6
		1.9368	4	$\bar{1}$ 3 7
		1.9347	3	1 3 7
		1.9300	3	7 1 6
		1.9262	3	$\bar{9}$ 1 2
12	1.9119	1.9161	3	7 3 1
		1.9097	4	$\bar{5}$ 1 8
		1.8985	2	5 1 8
5	1.8725	1.8850	5	7 3 2
		1.8513	2	0 0 10
6	1.8329	1.8247	3	2 4 5
		1.8214	3	$\bar{2}$ 2 9
		1.8165	2	$\bar{2}$ 0 10
9	1.8036	1.8024	2	$\bar{1}$ 1 10
		1.7951	5	$\bar{1}$ 3 8
		1.7572	2	6 4 0
		1.7415	2	$\bar{9}$ 1 5
		1.7376	2	$\bar{3}$ 1 10
12	1.7236	1.7313	3	3 1 10
		1.7276	2	$\bar{6}$ 4 2
		1.7256	2	3 3 8
		1.7198	2	$\bar{5}$ 3 7
		1.7132	2	$\bar{7}$ 3 5
8	1.6921	1.6996	4	$\bar{7}$ 1 8
		1.6886	3	7 1 8
		1.6704	2	2 2 10
17	1.6448	1.6529	5	9 3 0
		1.6501	2	$\bar{10}$ 2 2
		1.6471	2	$\bar{9}$ 3 1
		1.6453	4	$\bar{2}$ 4 7
		1.6331	2	3 5 2
		1.6287	2	$\bar{9}$ 3 2
11	1.6140	1.6247	2	$\bar{5}$ 1 10
		1.6187	2	$\bar{5}$ 3 8
		1.6158	3	8 0 8
		1.6109	2	$\bar{1}$ 5 4
		1.6035	2	$\bar{3}$ 5 3
13	1.5644	1.5783	2	$\bar{10}$ 2 4
		1.5750	2	6 0 10
		1.5720	4	10 2 4
		1.5680	2	0 2 11
		1.5593	5	$\bar{9}$ 3 4
		1.5535	2	2 4 8
		1.5437	2	$\bar{8}$ 4 2
		1.5181	2	$\bar{8}$ 4 3
8	1.5076	1.5132	4	8 2 8
		1.5057	2	4 3 10
		1.5002	2	5 1 11
14	1.4758	1.4793	5	4 2 11
		1.4761	2	5 5 4
		1.4708	2	3 1 12
		1.4610	3	6 4 7
6	1.4345	1.4404	2	$\bar{11}$ 1 6
		1.4325	4	7 5 1
7	1.4116	1.4168	3	$\bar{4}$ 4 9
		1.4112	2	10 2 7
8	1.3923	1.3980	2	$\bar{7}$ 1 11
		1.3939	3	11 3 3
		1.3927	2	8 4 6
		1.3900	2	10 4 0
		1.3798	2	$\bar{1}$ 5 8
		1.3736	2	10 4 2
		1.3710	2	$\bar{11}$ 3 4
6	1.3676	1.3665	4	$\bar{13}$ 1 2

good agreement with the pattern calculated from the structure determination. Unit-cell parameters refined from the powder data using *JADE 2010* with whole pattern fitting are $a = 18.174(5)$, $b = 8.635(5)$, $c = 18.485(5)$ Å, $\beta = 90.433(7)°$ and $V = 2901(2)$ Å^3.

The Rigaku *CrystalClear* software package was used for processing the structure data, including the

TABLE 3. Data collection and structure refinement details for juansilvaite.

Diffractometer	Rigaku R-Axis Rapid II
X-ray radiation / power	MoKα ($\lambda = 0.71075$ Å)/50 kV, 40 mA
Temperature	293(2) K
Structural formula	Na$_5$(Al$_{2.39}$Fe$_{0.61}$)[AsO$_3$(OH)]$_4$[AsO$_2$(OH)$_2$]$_2$(SO$_4$)$_2$·4H$_2$O
Space group	$C2/c$
Unit-cell dimensions	$a = 18.1775(13)$ Å
	$b = 8.6285(5)$ Å
	$c = 18.5138(13)$ Å
	$\beta = 90.389(6)°$
V	2903.7(3) Å^3
Z	4
Density (for above formula)	3.018 g cm^{-3}
Absorption coefficient	7.552 mm^{-1}
$F(000)$	2543.7
Crystal size (μm)	$80 \times 60 \times 10$
θ range	3.13 to 25.03°
Index ranges	$-21 \leq h \leq 21, -8 \leq k \leq 10, -22 \leq l \leq 22$
Reflections collected / unique	12,559/2524; $R_{int} = 0.066$
Reflections with $F > 4\sigma(F)$	2040
Completeness to $\theta = 25.03°$	98.7%
Max. and min. transmission	0.928 and 0.583
Refinement method	Full-matrix least-squares on F^2
Parameters/restraints	263/10
Goof	1.049
Final R indices [$F_o > 4\sigma(F)$]	$R_1 = 0.0382, wR_2 = 0.0786$
R indices (all data)	$R_1 = 0.0515, wR_2 = 0.0848$
Largest diff. peak/hole	$+0.99/-0.85$ e/A^3

*$R_{int} = \Sigma|F_o^2 - F_o^2(\text{mean})|/\Sigma[F_o^2]$. Goof $= S = \{\Sigma[w(F_o^2 - F_c^2)^2]/(n-p)\}^{1/2}$. $R_1 = \Sigma||F_o| - |F_c||/\Sigma|F_o|$. $wR_2 = \{\Sigma[w(F_o^2 - F_c^2)^2]/\Sigma[w(F_o^2)^2]\}^{1/2}$; $w = 1/[\sigma^2(F_o^2) + (aP)^2 + bP]$ where a is 0.0472, b is 28.6477 and P is $[2F_c^2 + \text{Max}(F_o^2, 0)]/3$.

application of an empirical multi-scan absorption correction using *ABSCOR* (Higashi, 2001). The structure was solved using *SIR2011* (Burla *et al*, 2012). *SHELXL-97* (Sheldrick, 2008) was used for the refinement of the structure. The Al1 and Al2 sites were refined with joint occupancy by Al and Fe, yielding a total for the two sites of Al$_{2.39}$Fe$_{0.61}$ apfu (46.9 electrons pfu), close to the Al$_{2.28}$Fe$_{0.50}$Mn$_{0.21}$ apfu (47.9 epfu) indicated by the empirical formula. A difference Fourier synthesis located all H atom positions, which were then refined with soft restraints of 0.82(3) Å on the O–H distances and 1.30(3) Å on the H–H distances and with the U_{eq} of each H of the OH groups set to 1.5 times that of the donor O atom and the U_{eq} of each H of the H$_2$O groups set to 1.2 times that of the donor O atom. Data collection and refinement details are given in Table 3, atom coordinates and displacement parameters in Table 4, selected bond distances in Table 5 and a bond valence analysis in Table 6.

Discussion

In the structure of juansilvaite (Fig. 3), Al1O$_6$ and Al2O$_5$(H$_2$O) octahedra and As1O$_3$(OH), As2O$_3$(OH) and As3O$_2$(OH)$_2$ tetrahedra share O vertices, yielding a layer parallel to {001} in which octahedra link only to tetrahedra, and not to other octahedra. Na1 and Na2 cations peripheral to the layers and Na3 cations within cavities in the layer form bonds to the vertices of the octahedra and tetrahedra in the layers. Na1 and Na2 also form bonds to an SO$_4$ tetrahedron in between the layers and both Na1 and Na3 bond to an otherwise isolated H$_2$O group (OW18).

The structure of juansilvaite is unique and we are unaware of any other structure to which it is very similar. The topology of the layer of alternating octahedra and tetrahedra also appears to be unique. Adjacent Al1 and Al2 octahedra are triple-linked to one another across adjacent faces by the three different As tetrahedra (As1, As2 and As3).

TABLE 4. Atom coordinates and displacement parameters (Å^2) for juansilvaite.

	x/a	y/b	z/c	U_{eq}	U^{11}	U^{22}	U^{33}	U^{23}	U^{13}	U^{12}
Na1	0.98040(14)	0.5486(3)	0.39677(15)	0.0281(6)	0.0294(15)	0.0268(17)	0.0279(15)	0.0031(12)	−0.0022(11)	−0.0043(12)
Na2	0.75160(14)	0.6574(3)	0.37425(14)	0.0254(6)	0.0243(15)	0.0187(15)	0.0332(16)	−0.0005(12)	0.0075(11)	−0.0011(11)
Na3	0	0.2038(5)	0.25	0.0316(10)	0.030(2)	0.020(2)	0.045(3)	0	0.0051(18)	0
Al1*	0.5	0.2932(2)	0.25	0.0134(8)	0.0123(12)	0.0122(13)	0.0158(13)	0	−0.0006(8)	0
Al2*	0.74706(8)	0.29047(18)	0.31201(8)	0.0136(6)	0.0113(9)	0.0112(9)	0.0182(9)	−0.0012(7)	−0.0010(6)	−0.0004(6)
As1	0.65145(3)	0.47862(7)	0.19865(3)	0.01412(19)	0.0129(3)	0.0118(4)	0.0177(4)	0.0008(3)	−0.0001(2)	0.0005(3)
As2	0.86684(3)	0.53651(8)	0.24115(3)	0.01380(19)	0.0117(3)	0.0135(4)	0.0162(4)	−0.0007(3)	−0.0003(2)	−0.0001(3)
As3	0.59673(3)	0.38975(8)	0.39168(3)	0.0162(2)	0.0158(4)	0.0137(4)	0.0191(4)	−0.0012(3)	−0.0006(2)	−0.0020(3)
S	0.85405(8)	0.60420(18)	0.51056(8)	0.0126(3)	0.0184(8)	0.0090(8)	0.0104(8)	−0.0020(6)	−0.0008(6)	0.0028(6)
O1	0.7844(3)	0.5206(6)	0.4960(3)	0.0378(13)	0.030(3)	0.040(4)	0.043(3)	−0.013(3)	−0.012(2)	0.003(3)
O2	0.8736(3)	0.6977(6)	0.4461(3)	0.0399(14)	0.065(4)	0.026(3)	0.028(3)	0.004(2)	0.011(3)	0.005(3)
O3	0.9146(2)	0.4918(5)	0.5242(3)	0.0261(11)	0.025(3)	0.021(3)	0.032(3)	−0.001(2)	−0.002(2)	0.005(2)
O4	0.8462(2)	0.7086(6)	0.5743(2)	0.0262(11)	0.025(3)	0.028(3)	0.025(3)	−0.002(2)	−0.0009(19)	0.004(2)
O5	0.6810(2)	0.6538(5)	0.2231(2)	0.0174(10)	0.017(2)	0.013(2)	0.022(2)	−0.0013(19)	0.0025(17)	0.0008(18)
O6	0.5671(2)	0.4601(5)	0.2326(2)	0.0157(9)	0.013(2)	0.012(2)	0.022(2)	0.0022(19)	0.0022(17)	0.0004(18)
O7	0.7097(2)	0.3320(5)	0.2166(2)	0.0167(10)	0.016(2)	0.013(2)	0.021(2)	−0.0025(19)	−0.0032(17)	0.0004(18)
OH8	0.6445(3)	0.4856(5)	0.1063(2)	0.0225(11)	0.032(3)	0.016(3)	0.020(3)	0.001(2)	−0.0016(19)	−0.003(2)
H8	0.639(4)	0.401(5)	0.091(4)	0.034						
O9	0.9320(2)	0.6386(5)	0.2827(2)	0.0152(9)	0.016(2)	0.013(2)	0.017(2)	−0.0027(18)	−0.0033(17)	−0.0014(18)
O10	0.8199(2)	0.6264(5)	0.1758(2)	0.0184(10)	0.016(2)	0.020(3)	0.019(2)	−0.001(2)	−0.0010(17)	0.0055(19)
O11	0.8146(2)	0.4617(5)	0.3065(2)	0.0161(10)	0.019(2)	0.012(2)	0.018(2)	−0.0006(19)	0.0033(17)	−0.0028(18)
OH12	0.9140(2)	0.3925(6)	0.1968(2)	0.0226(11)	0.021(3)	0.026(3)	0.021(3)	−0.003(2)	−0.0022(18)	0.000(2)
H12	0.886(3)	0.352(8)	0.169(3)	0.034						
O13	0.5352(2)	0.2821(5)	0.3489(2)	0.0161(10)	0.014(2)	0.012(2)	0.021(2)	−0.0029(19)	−0.0019(17)	−0.0059(18)
O14	0.6765(2)	0.4339(5)	0.3524(2)	0.0167(10)	0.013(2)	0.017(2)	0.020(2)	−0.0020(19)	0.0003(17)	−0.0021(18)
OH15	0.6129(3)	0.3062(6)	0.4731(3)	0.0280(11)	0.043(3)	0.023(3)	0.018(3)	−0.001(2)	−0.005(2)	−0.006(2)
H15	0.613(4)	0.213(4)	0.469(4)	0.042						
OH16	0.5560(3)	0.5631(6)	0.4118(3)	0.0302(12)	0.022(3)	0.014(3)	0.055(3)	−0.004(2)	0.004(2)	0.001(2)
H16	0.593(3)	0.616(8)	0.414(4)	0.045						
OW17	0.7821(3)	0.2605(6)	0.4111(2)	0.0240(11)	0.026(3)	0.019(3)	0.027(3)	−0.004(2)	−0.003(2)	0.003(2)
H17a	0.787(4)	0.327(5)	0.443(3)	0.029						
H17b	0.779(4)	0.179(4)	0.432(3)	0.029						
OW18	0.9475(3)	0.2886(6)	0.3710(3)	0.0267(11)	0.021(3)	0.024(3)	0.036(3)	0.000(2)	−0.003(2)	−0.002(2)
H18a	0.953(3)	0.207(5)	0.392(4)	0.032						
H18b	0.9029(17)	0.294(8)	0.364(4)	0.032						

* Occupancies: Al1/Fe1: 0.775/0.225(10), Al2/Fe2: 0.803/0.197(7)

TABLE 5. Selected bond distances (Å) for juansilvaite.

Na1–OW18	2.370(6)	Na2–O4	2.329(5)	Al1–O6(×2)	1.916(4)	As1–O5	1.666(4)	As3–O13	1.653(4)
Na1–O9	2.411(5)	Na2–O7	2.368(5)	Al1–O9(×2)	1.919(4)	As1–O6	1.668(4)	As3–O14	1.670(4)
Na1–O13	2.418(5)	Na2–O14	2.396(5)	Al1–O13(×2)	1.938(4)	As1–O7	1.681(4)	As3–OH15	1.695(5)
Na1–O3	2.422(5)	Na2–O11	2.399(5)	<Al1–O>	1.924	As1–OH8	1.714(5)	As3–OH16	1.711(5)
Na1–O2	2.506(6)	Na2–O2	2.602(6)			<As1–O>	1.682	<As3–O>	1.682
Na1–O3	2.697(5)	Na2–O1	2.610(6)	Al2–O5	1.880(4)				
Na1–OH12	2.924(5)	<Na2–O>	2.451	Al2–O10	1.882(4)	As2–O9	1.661(4)	S–O1	1.481(5)
<Na1–O>	2.535			Al2–O7	1.922(4)	As2–O10	1.667(4)	S–O2	1.486(5)
		Na3–O6(×2)	2.454(5)	Al2–O11	1.925(4)	As2–O11	1.673(4)	S–O3	1.487(5)
		Na3–OH12(×2)	2.459(5)	Al2–O14	1.936(4)	As2–OH12	1.721(5)	S–O4	1.493(5)
		Na3–OW18(×2)	2.548(5)	Al2–OW17	1.955(5)	<As2–O>	1.681	<S–O>	1.487
		<Na3–O>	2.487	<Al2–O>	1.917				

Hydrogen bonds

D–H⋯A	D–H	H⋯A	D⋯A	<DHA
OH8–H8⋯O2	0.79(3)	1.89(3)	2.686(7)	180(9)
OH12–H12⋯O4	0.80(3)	1.97(4)	2.717(6)	157(8)
OH15–H15⋯O3	0.81(3)	1.84(4)	2.620(7)	162(8)
OH16–H16⋯O4	0.81(3)	1.89(4)	2.665(7)	160(8)
OW17–H17a⋯O1	0.83(3)	1.94(3)	2.740(7)	163(6)
OW17–H17b⋯OH8	0.81(3)	2.29(6)	2.741(7)	116(6)
OW18–H18a⋯OH16	0.81(3)	2.28(5)	2.868(7)	130(6)
OW18–H18b⋯none				

TABLE 6. Bond-valence analysis for juansilvaite. Values are expressed in valence units.

	O1	O2	O3	O4	O5	O6	O7	OH8	O9	O10	O11	OH12	O13	O14	OH15	OH16	OW17	OW18	Σ_c
Na1		0.15	0.19 0.09						0.19			0.05	0.19					0.21	1.07
Na2	0.15	0.11		0.24			0.22					0.20		0.20					1.12
Na3						0.17 ×2→						0.17 ×2→						0.13 ×2→	0.94
Al1						0.50 ×2→			0.49 ×2→				0.47 ×2→						2.91
Al2					0.54		0.48			0.54	0.48			0.46			0.44		2.94
S	1.47	1.45	1.45	1.42															5.80
As1					1.31	1.31	1.26	1.15											5.04
As2									1.33	1.31	1.29	1.13							5.06
As3													1.36	1.30	1.21	1.16			5.04
H8		0.21						0.79											1.00
H12				0.20								0.80							1.00
H15			0.24												0.76				1.00
H16				0.22												0.78			1.00
H17a	0.20																0.80		1.00
H17b								0.19									0.81		1.00
H18a																0.16		0.84	1.00
H18b																		1.00	1.00
Σ_a	1.82	1.92	1.96	2.08	1.85	1.97	1.96	2.13	2.01	1.85	1.97	2.15	2.02	1.96	1.97	2.10	2.05	2.19	

Multiplicities indicated by ×2→; Na^+–O bond-valence parameters from Wood and Palenik (1999); Al^{3+}–O, Fe^{3+}–O, As^{5+}–O and S^{6+}–O from Brown and Altermatt (1985); hydrogen-bond strengths based on O···O bond lengths also from Brown and Altermatt (1985).
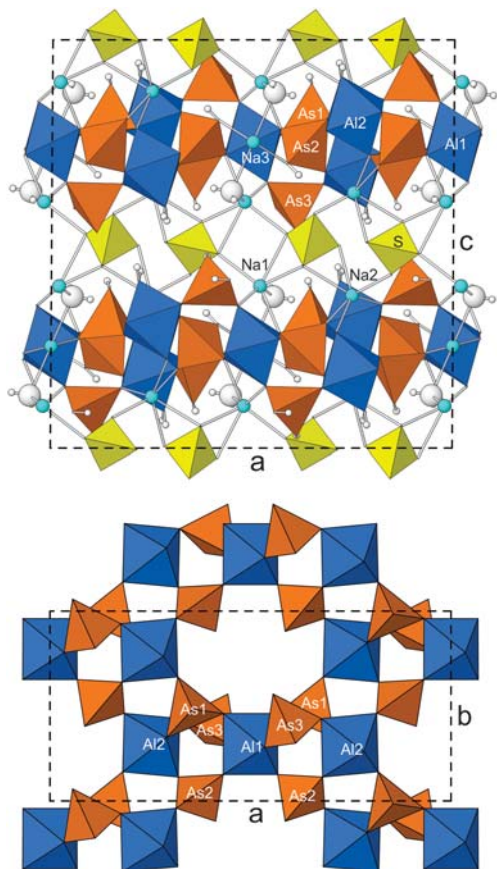
Fig. 3. The crystal structure of juansilvaite viewed along [010] (*top*) and layer of Al1O$_6$ and Al2O$_5$(H$_2$O) octahedra and As1O$_3$(OH), As2O$_3$(OH) and As3O$_2$(OH)$_2$ tetrahedra viewed along [001] (*bottom*). The unit cell is shown by dashed lines. Note that, in the lower image, all of the polyhedra constituting the 'double lantern unit' are labelled.

Adjacent Al2 octahedra are double-linked to one another by As1 and As2 tetrahedra. There are no Al1 octahedra adjacent to one another. The most distinctive portion of the layer linkage consists of two successive triple linkages between Al2–Al1–Al2 octahedra corresponding to a [Al$_3$(AsO$_4$)$_6$] unit with the same local topology as the 'double lantern unit' in the structures of the sulfates coquimbite, aluminocoquimbite (Demartin *et al.*, 2010) and paracoquimbite (Majzlan *et al.*, 2010), and the phosphate taranakite (Dick *et al.*, 1998; Kampf *et al.*, 2013c). Among arsenates, an infinite chain with this triple linkage is found in the structure of kaatialaite (Boudjada and Guitel, 1981).

References

Boudjada, A. and Guitel, J.C. (1981) Structure cristalline d'un orthoarsénate acide de fer(III) pentahydraté: Fe(H$_2$AsO$_4$)$_3$·5H$_2$O. *Acta Crystallographica*, **B37**, 1402–1405.

Brown, I.D. and Altermatt, D. (1985) Bond–valence parameters from a systematic analysis of the inorganic crystal structure database. *Acta Crystallographica*, **B41**, 244–247.

Burla, M. C., Caliandro, R., Camalli, M., Carrozzini, B., Cascarano, G.L., Giacovazzo, C., Mallamo, M., Mazzone, A., Polidori, G. and Spagna, R. (2012) *SIR2011*: a new package for crystal structure determination and refinement. *Journal of Applied Crystallography*, **45**, 357–361.

Cameron, E.M., Leybourne, M.I. and Palacios, C. (2007) Atacamite in the oxide zone of copper deposits in northern Chile: involvement of deep formation waters? *Mineralium Deposita*, **42**, 205–218.

Demartin, F., Castellano, C., Gramaccioli, C.M. and Campostrini, I. (2010) Aluminum-for-iron substitution, hydrogen bonding and a novel structure type in coquimbite-like minerals. *The Canadian Mineralogist*, **48**, 323–333.

Dick, S., Goßner, U., Weiß, A., Robl, C., Großmann, G., Ohms, G. and Zeiske, T. (1998) Taranakite – the mineral with the longest crystallographic axis. *Inorganica Chimica Acta*, **269**, 47–57.

Gutiérrez, H. (1975) *Informe sobre una rápida visita a la mina de arsénico nativo, Torrecillas*. Instituto de Investigaciones Geológicas, Iquique, Chile.

Higashi, T. (2001) *ABSCOR*. Rigaku Corporation, Tokyo.

Kampf, A.R., Sciberras, M.J., Williams, P.A., Dini, M. and Molina Donoso, A.A. (2013*a*) Leverettite from the Torrecillas mine, Iquique Provence, Chile: the Co-analogue of herbertsmithite. *Mineralogical Magazine*, **77**, 3047–3054.

Kampf, A.R., Nash, B.P., Dini, M. and Molina Donoso, A. A. (2013*b*) Magnesiokoritnigite, Mg(AsO$_3$OH)·H$_2$O, from the Torrecillas mine, Iquique Province, Chile: the Mg-analogue of koritnigite. *Mineralogical Magazine*, **77**, 3081–3092.

Kampf, A.R., Mills, S.J., Nash, B.P., Housley, R.M., Rossman, G.R. and Dini, M. (2013*c*) Camaronesite, [Fe^{3+}(H$_2$O)$_2$(PO$_3$OH)]$_2$(SO$_4$)·1–2H$_2$O, a new phosphate-sulfate from the Camarones Valley, Chile,

structurally related to taranakite. *Mineralogical Magazine*, **77**, 453–465.

Kampf, A.R., Nash, B.P., Dini, M. and Molina Donoso, A. A. (2014*a*) Torrecillasite, NaAs,Sb)$_4^{3+}$O$_6$Cl, a new mineral from the Torrecillas mine, Iquique Province, Chile: description and crystal structure. *Mineralogical Magazine*, **78**, 747–755.

Kampf, A.R., Mills, S.J., Hatert, F., Nash, B.P., Dini, M. and Molina Donoso, A.A. (2014*b*) Canutite, NaMn$_3$ [AsO$_4$]$_2$[AsO$_2$(OH)$_2$], a new protonated alluaudite–group mineral from the Torrecillas mine, Iquique Province, Chile. *Mineralogical Magazine*, **78**, 787–795.

Kampf, A.R., Nash, B., Dini, M. and Molina Donoso, A. A. (2015) Juansilvaite, IMA 2015-080. CNMNC Newsletter No. 28, December 2015, page 1863; *Mineralogical Magazine*, **79**, 1859–1864.

Kampf, A.R., Nash, B.P., Dini, M. and Molina Donoso, A.A. (2016*a*) Chongite, Ca$_3$Mg$_2$(AsO$_4$)$_2$(AsO$_3$OH)$_2$·4H$_2$O, a new arsenate member of the hureaulite group from the Torrecillas mine, Iquique Province, Chile. *Mineralogical Magazine*, **80**, 1255–1263.

Kampf, A.R., Nash, B.P., Dini, M. and Molina Donoso, A.A. (2016*b*) Gajardoite, KCa$_{0.5}$As$_4^{3+}$O$_6$Cl$_2$·5H$_2$O, a new

mineral related to lucabindiite and torrecillasite from the Torrecillas mine, Iquique Province, Chile. *Mineralogical Magazine*, **80**, 1265–1272.

Mandarino, J.A. (2007) The Gladstone–Dale compatibility of minerals and its use in selecting mineral species for further study. *The Canadian Mineralogist*, **45**, 1307–1324.

Majzlan, J., Đorđević, T., Kolitsch, U. and Schefer, J. (2010) Hydrogen bonding in coquimbite, nominally Fe$_2$(SO$_4$)$_3$·9H$_2$O, and the relationship between coquimbite and paracoquimbite. *Mineralogy and Petrology*, **100**, 241–248.

Pouchou, J.-L. and Pichoir, F. (1991) Quantitative analysis of homogeneous or stratified microvolumes applying the model "PAP." Pp. 3l–75 in: *Electron Probe Quantitation* (K.F.J. Heinrich and D.E. Newbury, editors). Plenum Press, New York.

Sheldrick, G.M. (2008) A short history of *SHELX*. *Acta Crystallographica*, **A64**, 112–122.

Wood, R.M. and Palenik, G.J. (1999) Bond valence sums in coordination chemistry. Sodium-oxygen complexes. *Inorganic Chemistry*, **38**, 3926–3930.